Brighten-and-Colorize: A Decoupled Network for Customized Low-Light Image Enhancement

Chenxi Wang
Sun Yat-sen University
Shenzhen, Guangdong, China
wangchx67@mail2.sysu.edu.cn

Zhi Jin*
Sun Yat-sen University
Shenzhen, Guangdong, China
jinzh26@mail2.sysu.edu.cn

Figure 1: The enhanced results of the proposed method. (a) Compared with the results of current methods [37, 41, 45], which suffer from chromatic aberration, the proposed method reaches enhancement with accurate color. (b) The proposed method achieves customized enhancement based on reference images. (c) The proposed method can adjust the saturations of the enhanced results.

ABSTRACT

Low-Light Image Enhancement (LLIE) aims to improve the perceptual quality of an image captured in low-light conditions. Generally, a low-light image can be divided into lightness and chrominance components. Recent advances in this area mainly focus on the refinement of the lightness, while ignoring the role of chrominance. It easily leads to chromatic aberration and, to some extent, limits the diverse applications of chrominance in customized LLIE. In this work, a "brighten-and-colorize" network (called BCNet), which introduces image colorization to LLIE, is proposed to address the above issues. BCNet can accomplish LLIE with accurate color and simultaneously enables customized enhancement with varying saturations and color styles based on user preferences. Specifically, BCNet regards LLIE as a multi-task learning problem: brightening and colorization. The brightening sub-task aligns with other conventional LLIE methods to get a well-lit lightness. The colorization sub-task is accomplished by regarding the chrominance of the low-light image as color guidance like the user-guide image colorization. Upon completion of model training, the color guidance (i.e., input low-light chrominance) can be simply manipulated by users to acquire customized results. This customized process is optional and, due to its decoupled nature, does not compromise the structural and detailed information of lightness. Extensive experiments on the commonly used LLIE datasets show that the proposed method achieves both State-Of-The-Art (SOTA) performance and user-friendly customization.

*Corresponding author.

CCS CONCEPTS

• **Computing methodologies** → **Computer vision**; **Image processing**.

KEYWORDS

Low-light image enhancement, Image colorization, Customized enhancement

1 INTRODUCTION

Low-Light Image Enhancement (LLIE) is an important but challenging task in computer vision. It can not only improve the visual quality, but also be helpful for other high-level computer vision tasks (e.g., face detection [42], action recognition [27], and object detection [31]). Until now, many traditional methods [11, 28, 29] and learning-based methods [22, 37, 39, 41, 43, 45, 46, 51, 52] have been proposed to enhance low-light images. However, most of them mainly focus on improving the quality of the lightness, which easily leads to serious loss of chrominance information and unpleasant visual results. Although some works try to apply additional constraints on chrominance information (e.g., the vectors of RGB channels [37]), they still hardly handle chrominance information well (as shown in Fig. 1 (a)). On the other hand, chrominance plays an important role in customized enhancement, however, recent customized methods [14, 34, 36, 47, 57] do not notice this problem. iUP-Enhancer [57] achieved chrominance customization by leveraging histograms in HSV color space, while the histograms as global information hardly guarantee local consistency. In summary, existing (customized) LLIE methods do not pay enough attention to the importance of chrominance information.

Meanwhile, image colorization, as an active research field that aims to predict lost chrominance information on the given lightness, has two key challenges: 1) *how to ensure boundaries of the generated chrominance*, 2) *how to solve the problem that one object can be filled by multiple colors (e.g., a balloon can be colorized red or blue).* Some image colorization methods tackle these problems by introducing semantic information [33, 54], which can provide the boundaries or object information, and the user interactions (e.g. color strokes [50] or reference image [6, 23]), which are helpful for generating the certain colors. However, we observe that although the chrominance of low-light image is unsaturated, it contains both boundary information and some color hints.

Hence, we novelly propose to regard the chrominance prediction in LLIE as a colorization problem, which takes the low-light chrominance as a guidance to recover proper colors. In this way, LLIE is decoupled into the brightening and colorization sub-tasks. Since the input of the colorization process is usually carried out on grey images under normal light, an intuitive implementation is to first brighten the low-light lightness and then colorize it. However, this two-step approach is tedious and lacks information interactions between two sub-tasks. In this work, a new "brighten-and-colorize"

paradigm, called BCNet is proposed. BCNet adopts multi-task learning architecture, which contains one encoder and two task-specific decoders. The encoder takes the low-light lightness as the input, while the two task-specific decoders aim to output predicted lightness and chrominance, respectively. By training two sub-tasks simultaneously, the brightening sub-task can provide information of normal-light lightness to the colorization sub-task. Besides, the color classification loss [48], which transforms colorization to a classification task, is introduced to relieve color vanishment in the colorization sub-task.

Since the chrominance of the low-light image serves as color guidance for colorization, users can modify it to generate customized results in the testing phase. In our work, we introduce two customized operations. Firstly, users can change the color style of the guidance based on a reference image, resulting in diverse color styles (see Fig. 1 (b)). Secondly, users can adjust the saturation of the guidance coarsely to achieve the enhancement with different saturations (see Fig. 1 (c)). Note that the key process of customized enhancement in this work is to generate customized color guidance for the colorization sub-task, some simple non-learning operators are sufficient to produce pleasing results. Meanwhile, benefiting from the decoupled nature, the details of the lightness component can be preserved well during any customized processes.

To sum up, our contributions are four folds: **1) We decouple LLIE into brightening and colorization sub-tasks by introducing image colorization. 2) A multi-task learning architecture called BCNet is proposed to implement this decoupled enhancement. 3) Based on the property of the colorization sub-task, we provide a new solution for customized LLIE. 4) Extensive experiments on popular LLIE datasets demonstrate the proposed method reaches SOTA performance and performs well on customized LLIE.**

2 RELATED WORK

2.1 Low-Light Image Enhancement

Traditional low-light image enhancement (LLIE) methods can be broadly categorized into two types: Histogram Equalization (HE)-based methods [28] and Retinex-based methods [11, 29]. HE-based methods aim to flatten the histograms of low-light images, while Retinex-based methods attempt to decompose low-light images into illumination and reflectance components. However, these traditional methods often struggle with noise and color. In recent years, Deep Neural Networks (DNNs) have shown great potential for image enhancement [7, 9, 10, 12, 13, 19, 22, 40, 53]. The first Convolutional Neural Network (CNN) architecture designed for LLIE was proposed by Lore *et al.* [22], and since then, several other CNN-based architectures [3, 12, 13, 40] have been proposed. To achieve more realistic results, Retinex theory has been incorporated into DNNs [39, 43, 51, 52]. Methods in [5, 37, 53] apply an additional constraint on color information. Besides, many unsupervised methods [5, 8, 21, 24] have been proposed to eliminate the requirement of paired training data. However, these methods often do not make optimal use of chrominance.

Another line of LLIE methods aims to achieve customized enhancement to satisfy the different preferences of users. The first method to introduce customization to LLIE was PieNet [14], which
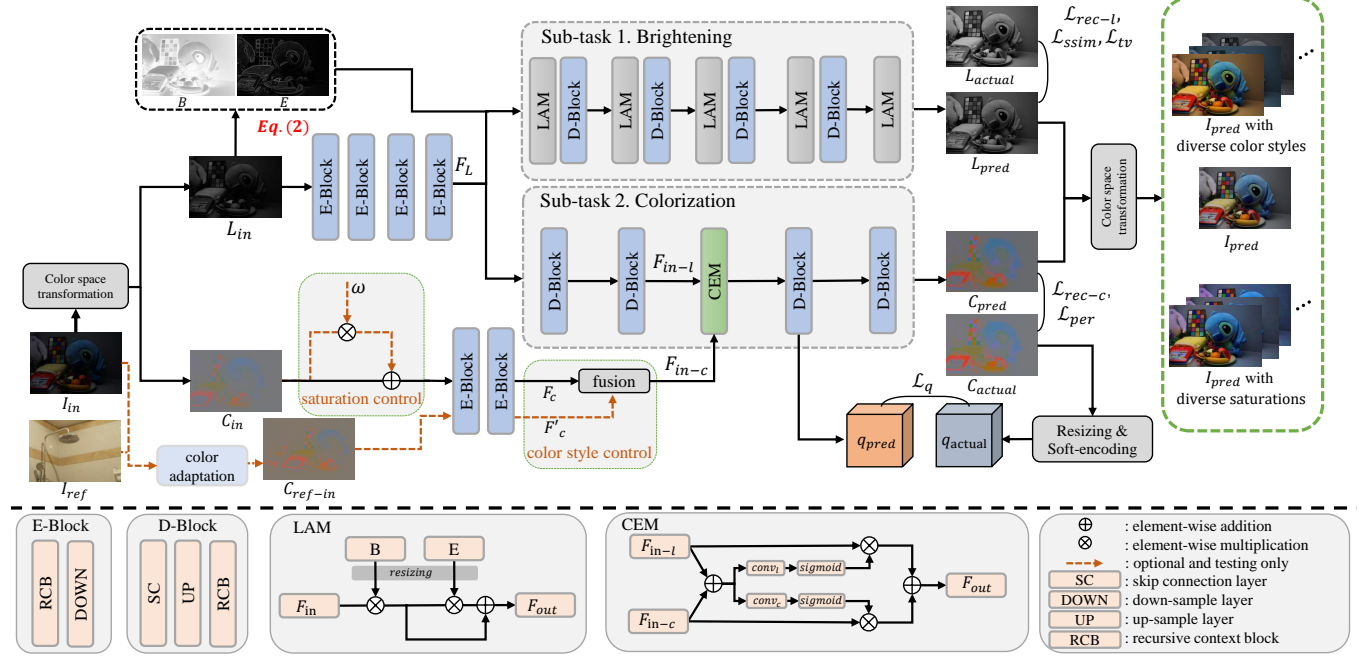
Figure 2: Framework of the proposed method. The proposed method adopts multi-task learning architecture, containing one encoder and two task-specific decoders. It implements two sub-tasks: brightening and colorization. After model training is completed, the input chrominance can be manipulated by users to achieve enhancement with diver styles and saturations.

achieved customized enhancement by extracting style vectors from reference images. TSFlow [36] introduced style vectors to normalizing flow [16] to obtain diverse results. However, these "black-box" processes may lead to poor flexibility for user customization. ReL-LIE [47] achieved enhancements with different brightness by introducing deep reinforcement learning, but it ignores chrominance information. iUP-Enhancer [57] provided a "white-box" approach to accomplish customized enhancement by leveraging histogram information in the HSV color space. While histograms as a form of global information may hardly ensure local consistency. Compared to existing customized LLIE methods, BCNet provides a new perspective by using image colorization to achieve customization. This approach preserves lightness details well and allows for accurate chrominance.

2.2 Image Colorization

Image colorization techniques can be classified into two categories: automatic colorization and user-guided colorization. Automatic colorization [4, 17, 48] aims to colorize grayscale images without any external color guidance. Zhang *et al.* [48] transformed image colorization into a classification task to generate diverse colorization results. Kumar *et al.* [17] introduced transformer [35] to image colorization. However, automatic colorization methods often suffer from color ambiguity. To address this issue, user-guided image colorization methods were proposed. Zhang *et al.* [50] utilized color strokes as color guidance, while He *et al.* [6], Lu *et al.* [23], and Yin *et al.* [44] used exemplar images as color references. Moreover, to achieve more precise colorization, some methods [33, 54] incorporated semantic information to provide object boundaries and

object-specific colorization. In this work, we present a user-guided colorization method that leverages the chrominance information of low-light images to provide not only color guidance but also object boundary information. We also introduce the concept of color classification [48] and apply both regression and classification constraints to achieve more robust colorization.

3 METHOD

3.1 "Brighten-and-Colorize"

To accomplish the "brighten-and-colorize" enhancement, we first decompose the image into lightness and chrominance. In widely used RGB color space, every single channel contains part of lightness and chrominance, which means they are inseparable in the RGB color space. Therefore, to separate lightness and chrominance, we transform the image from RGB color space to CIELAB color space, where the "L" channel represents lightness and the "AB" channels represent chrominance. Note that we follow the commonly used color space transform function in the image colorization field.

After decomposing the image, the LLIE task is decoupled into two sub-tasks: brightening and colorization. The brightening itself can be regarded as an LLIE problem that predicts lightness with well exposure and details. The colorization aims to predict realistic and accurate chrominance based on the normal-light lightness information and low-light chrominance like user-guide image colorization methods.

3.2 Network Architecture

In this sub-section, we present the details of the proposed method BCNet shown in Fig. 2. BCNet adopts multi-task learning architecture and contains an encoder and two task-specific decoders. Given a low-light image $I_{in} \in \mathbb{R}^{H \times W \times 3}$, we first decompose it into a lightness map $L_{in} \in \mathbb{R}^{H \times W \times 1}$ and a chrominance map $C_{in} \in \mathbb{R}^{H \times W \times 2}$. Then, the encoder takes L_{in} as input and two task-specific decoders output a predicted lightness $L_{pred} \in \mathbb{R}^{H \times W \times 1}$ and a predicted chrominance $C_{pred} \in \mathbb{R}^{H \times W \times 2}$, respectively. The constraints are applied with lightness of ground-truth $L_{actual} \in \mathbb{R}^{H \times W \times 1}$ and chrominance of ground-truth $C_{actual} \in \mathbb{R}^{H \times W \times 2}$. In the following parts, we illustrate the reasonability for adopting the multi-task learning design and the details of two task-specific decoders.

3.2.1 Multi-Task Encoder. The structure content of the lightness is essential for the brightening and colorization sub-tasks. It determines the network how to brighten and where to colorize. In this work, the brightening sub-task aims to recover the clear structure content of lightness, and the colorization sub-task predicts the lost chrominance based on the clear structure content. Due to different inputs, the two sub-tasks are not in the typical design of multi-task learning. However, when training the brightening sub-task, the encoder can learn the information of the clear structure content, which is necessary for the colorization sub-task. By sharing the same encoder, this necessary information for the colorization sub-task can be obtained from the brightening sub-task. Hence, it still can be regarded as a multi-task learning problem. Further, this design not only encourages the information interactions between two sub-tasks but also makes the network more efficient.

Referring to Fig. 2, the multi-task encoder takes the low-light lightness image as input and contains four encoding blocks (E-Block). Every encoding block consists of a Recursive Context Block (RCB) [45], which provides a more effective feature extraction, and a down-sample layer. In this way, we can extract the features F_L from L_{in} as:

$$F_L = Encoder(L_{in}) \tag{1}$$

Note that the output of every encoding block is transmitted to the corresponding decoding block in two sub-tasks by skip-connection layers.

3.2.2 Lightness Decoder. The lightness decoder is adopted in the brightening sub-task. It contains four decoding blocks (D-Block) and five Lightness Adjustment Modules (LAMs). Every decoding block consists of a skip-connection layer, an up-sample layer, and an RCB. The LAM is proposed for guiding the network to improve contrast and preserve better details. Empirically, the darker regions of a low-light image need to be brightened more than brighter regions, and the edges information is essential for an enhanced image. Hence, LAM first takes the inverted map B of L_{in} as the attention prior to indicate where needs more contrast improvement. Then, it utilizes the edge map E of L_{in} to help preserve edges. As shown in Fig. 2, the LAM can be formulated as:

$$B = 1 - L_{in}, E = edge(L_{in}) \tag{2}$$

$$F_{out} = F_{in} \times \psi(B) \times (1 + \psi(E)) \tag{3}$$

where F_{in} and F_{out} are input and output features, respectively. $\psi(.)$ represents resizing operation (bilinear is adopted in this work). *edge*
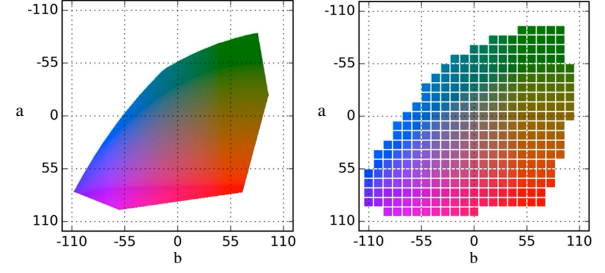

Figure 3: The quantization operation [48] in CIELAB color space. The continuous colors (left) are quantized to 313 discrete colors (right) with a grid size of 10.

denotes an edge extractor, which is a *sobel* operator with kernel size of 3. Then, the predicted lightness L_{pred} can be obtained by:

$$L_{pred} = Brightening(F_L, B, E) \tag{4}$$

3.2.3 Chrominance Decoder. The chrominance decoder is adopted in the colorization sub-task, which contains four decoding blocks and a Color Embedding Module (CEM).

Colorization by the low-light chrominance. As mentioned before, colorization is an ill-posed problem, since the color of a certain object is ambiguous. Existing image colorization methods address this issue through the user-guide strategy that introduces an exemplar image or color strokes as color hints. The exemplar image can offer a specific color style, and the color strokes provide approximate guidance. Besides, the colorization methods easily colorize one object beyond its boundary, and this problem can be relieved by introducing semantic information, which reflects the boundaries of objects, to the colorization process. However, different from the original image colorization tasks, in this work, the low-light images already contain part of the chrominance information. Although it is unsaturated, it can provide enough clues to help generate the proper chrominance. For example, the chrominance C_{in} in Fig. 2 is from the input low-light image, it still reflects the approximate color tone and shapes of the ground-truth chrominance C_{actual}.

Therefore, we utilize this information by embedding the features of C_{in} to the chrominance decoder. Inspired by [20], we regard features extracted from lightness and chrominance as multi-scale (i.e., multiple information sources) features and propose a CEM to accomplish feature fusion. As shown in Fig. 2, given the input features F_{in-l} extracted from L_{in} and F_{in-c} extracted from C_{in}, CEM first get the summation feature $\hat{F_{in}}$ of two features by element-wise addition as:

$$\hat{F_{in}} = F_{in-l} + F_{in-c} \tag{5}$$

Then, we calculate affinity matrices A_l, A_c, which are used to embed chrominance features to the colorization process, by two convolutional layers and *sigmoid* activations as:

$$A_l = sigmoid(conv_l(\hat{F_{in}})), A_c = sigmoid(conv_c(\hat{F_{in}})) \tag{6}$$

Finally, the output feature F_{out} of CEM is obtain by:

$$F_{out} = F_{in-l} \times A_l + F_{in-c} \times A_c \tag{7}$$

Colorization free from color vanishment. Regarding colorization as a regression task easily results in color vanishment. For example, the day sky is blue and the dusk sky is red, while the

reference images:
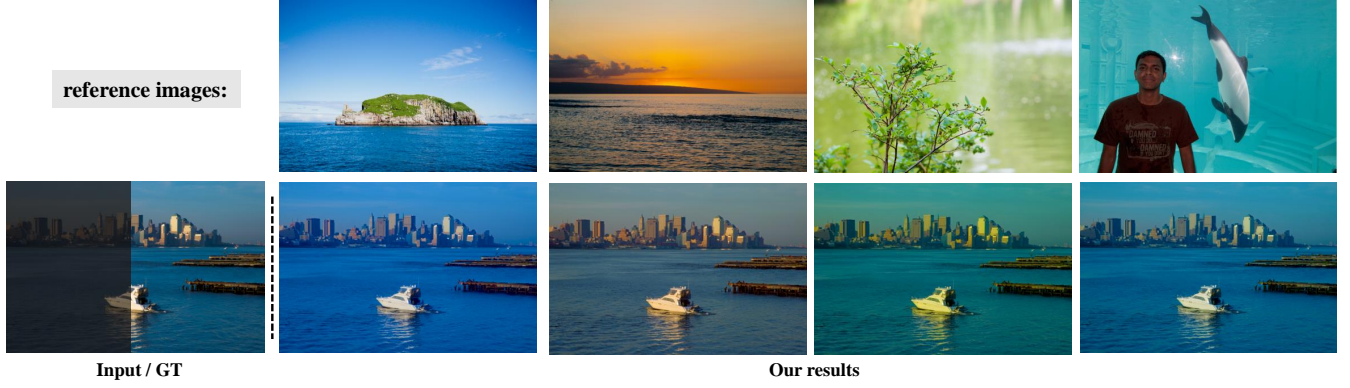
Input / GT　　　　　　　　　　　　　　　　　**Our results**

Figure 4: The visual results of color style control. It can be seen that the enhanced results have different color styles based on different reference images.

$\omega = 0$　　　　More saturated　　　　$\omega = 1$

Input / GT　　　　　　　　　　　　　　　　**Our results**

Figure 5: The visual results of saturation control. It can be seen that the result becomes more saturated as the value of ω goes up.

mean of red and blue is gray. To relieve this problem, we quantize entire colors in CIELAB color space to 313 categories with a grid size of 10 (as shown in Fig. 3) and calculate the classification loss followed by [48]. It is an effective solution for color vanishment. Note that the classification output $q_{pred} \in \mathbb{R}^{h \times w \times 313}$ hardly reaches the original size of the image limited by memory. We set h and w to a quarter of the original size. However, it may affect the enhanced result at the pixel-level. On the other hand, the quantized operation can also lead to performance degradation. Therefore, we apply constraints on color classification output and chrominance map simultaneously, which is helpful for generating various colors and more precise colors at pixel-level, respectively. The predicted chrominance map C_{pred} and color classification output q_{pred} can be expressed by:

$$C_{pred}, q_{pred} = Colorization(F_L, C_{in}) \quad (8)$$

3.3 Loss Functions

We apply different constraints in the brightening and colorization sub-tasks based on their different characteristics. For lightness losses, Charbonnier loss [18] is first applied as the reconstruct loss $\mathcal{L}_{rec-l}$ to supervise lightness reconstruction at pixel-level, which can be defined as:

$$\mathcal{L}_{rec-l} = \sqrt{\|L_{actual} - L_{pred}\|_2 + \epsilon^2} \quad (9)$$

where ϵ is set to 10^{-3} empirically. Then, the SSIM [38] loss $\mathcal{L}_{ssim}$ and total variation [2] loss $\mathcal{L}_{tv}$ are applied to get a better structural details. For chrominance losses, as analyzed in [48, 50], L2 loss is not robust for colorization due to the inherent multi-modal nature of colorization. In this work, we apply L1 loss as chrominance

reconstruction loss $\mathcal{L}_{rec-c}$, which is described as:

$$\mathcal{L}_{rec-c} = \|C_{actual} - C_{pred}\|_1 \quad (10)$$

Next, the perceptual loss $\mathcal{L}_{per}$, which constrains in features extracted from VGGNet[32], is adopted to get better visual results.

Then, color classification loss $\mathcal{L}_q$ is applied to get various colors. The $\mathcal{L}_q$ is defined as:

$$\mathcal{L}_q = \mathcal{H}(q_{actual}, q_{pred}) \quad (11)$$

where $\mathcal{H}(.)$ is a 2-D cross-entropy loss function. q_{actual} is obtained by soft-encoding resized C_{actual} as [48].

The total loss of BCNet $\mathcal{L}_{total}$ can be formulated as:

$$\begin{aligned} \mathcal{L}_{total} = &\lambda_1 \mathcal{L}_{rec-l} + \lambda_2 \mathcal{L}_{ssim} + \lambda_3 \mathcal{L}_{tv} + \\ &\lambda_4 \mathcal{L}_{rec-c} + \lambda_5 \mathcal{L}_{per} + \lambda_6 \mathcal{L}_q \end{aligned} \quad (12)$$

where $\lambda_1, \lambda_2, \lambda_3, \lambda_4, \lambda_5, \lambda_6$ are weigh factors and set to 1, 0.1, 0.01, 1, 0.01, 0.01, respectively.

3.4 Customized Enhancement

The chrominance of low-light images is served as color guidance to help the colorization sub-task. It provides two essential pieces of information: 1) boundaries information for guiding where to colorize, and 2) color hints for guiding what color to be used. When model training is completed, users can modify the color guidance to achieve customized enhancement. This process only needs to maintain the boundaries information of color guidance to ensure the position of predicted chrominance. Meanwhile, the lightness component is lossless after customized operations since the guidance only affects the colorization sub-task. In this work, two customized

(a) Input **(b) Reference** **(c) Color adaptation of (a) and (b)**

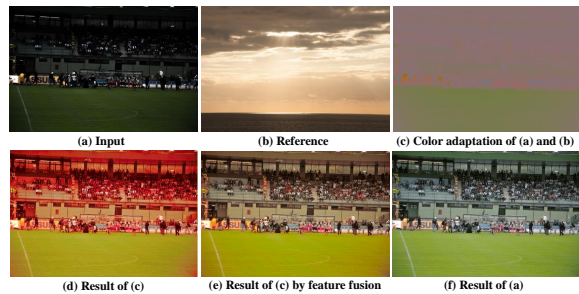**(d) Result of (c)** **(e) Result of (c) by feature fusion** **(f) Result of (a)**

Figure 6: The process of color style control. The input image (a) and reference image (b) first through a color adaptation module [30] to get customized color guidance (c). (d) is the result of directly embedding (c) to the colorization process, (e) is the result of embedding (c) to the colorization process with a feature fusion module, and (f) is the result of directly embedding the original chrominance of (a) to the colorization process. By comparing (d), (e), and (f), we can find the color style of (b) is transferred to (e) and the feature fusion module is helpful for keeping the color details.

operations, which achieve color style control (see Fig. 4) and color saturation control (see Fig. 5), are proposed as follows.

3.4.1 Color Style Control. To generate results with diverse color styles, the color hints provided by guidance can be modified. However, since the boundary information needs to be preserved, manually modifying them may be complicated. One effective solution is to introduce a reference image. There are many color style transfer works [6, 23, 44] that can transmit the color style from a reference image to the input image. In our case, since the modification is applied to the guidance, we do not need to explore a complex and accurate transfer. Therefore, we adopt a traditional non-learning color transfer method [30], which achieves color transfer by transforming images to an orthogonal color space (the detailed implementation can be found in supplementary materials), to obtain customized color guidance (as shown in Fig. 6 (c)). However, this traditional method may hardly perform well in some color details when the input and reference images are irrelevant (as shown in Fig. 6 (d)). To address this issue, we fuse the features F_c extracted from C_{in} into the features F_c' extracted from C_{ref-in} to retain the color details (as shown in Fig. 6 (e)). The fusion process is defined as $(1 - \gamma) \times F_c + \gamma \times F_c'$, where γ is a hyper-parameter that balances the two features and is set to 0.7 for testing and 0 for training.

3.4.2 Saturation Control. The color guidance provides what color should be used, besides, its intensity also can affect the saturation of output. To preserve the boundaries information, a simple amplified operation is designed as shown in "saturation control" of Fig. 2. The amplified color guidance is obtained by $C_{in} \times (1 + \omega)$, where ω is a hyper-parameter to control the saturation. The bigger ω represents the result is more saturated and colorful (see Fig. 5). Actually, ω can be any value, we empirically set $\omega \in [0, 1]$. When $\omega < 0$ or $\omega > 1$, the results may be over dull or saturated.

Note that the above customized operations are not involved in model training. They are optional and only run in the testing phase.
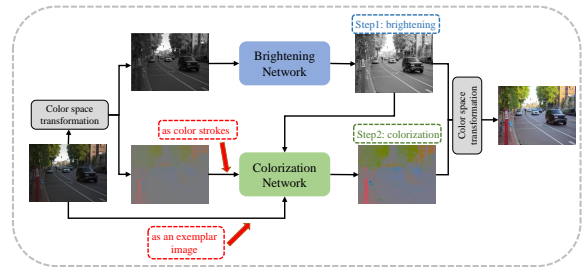

Figure 7: The illustration of the two-step "brighten-and-colorize". Note that the exemplar-based colorizer takes the low-light image as color hints and the stroke-based colorizer takes the chrominance of the low-light image as color hints.

4 EXPERIMENT

4.1 Datasets and Implementation Details

LOL-real [43] and MIT-Adobe-FiveK [1] (for short called FiveK) are adopted as our experimental datasets. LOL-real is captured in the real world by changing exposure time and ISO. It contains 689 pairs of low-/normal-light images for training and 100 pairs for testing. FiveK contains 5,000 raw images and corresponding five high-quality versions retouched by experts. The version retouched by expert C is adopted as the ground-truth and it is divided into 4,500 training pairs and 500 testing pairs following [37, 45].

BCNet is implemented in PyTorch and trained in an RTX2080Ti GPU with batch size of 8. The learning rate is initiated to 2.0×10^{-4} and a multi-step scheduler is adopted. Adam [15] with momentum of 0.9 is adopted as the optimizer. Input training images are randomly cropped to 256×256 and rotated by multiples of 90 degrees.

4.2 Comparison with Recent LLIE Methods

We compare BCNet with recent SOTA LLIE methods, which include DRD [39], Kind [52], Kind++ [51], MIRNet [46], EnGAN [8], Deep-UPE [37], DeepLPF [25], UEGAN [26], SGM [43], MIRNet-v2 [45], and SNR-Aware [41]. Note that we load the pre-trained parameters of EnGAN and retrain other methods on the same datasets.

Quantitative comparison. In this work, PSNR, SSIM [38], the $L_2 - distance$ in CIELAB color space ($\triangle E_{ab}$), LPIPS [49], and Color-Sensitive Error (CSE) [56] are employed as the evaluation matrices. Note that LPIPS measures the distance of high-level features between two images, and CSE measures the color difference between two images. We employ the ratio of our result as the unit of CSE following recent works [53, 55]. In general, the lower LPIPS, lower CSE, lower $\triangle E_{ab}$, higher SSIM, and higher PSNR values represent two images with more relative low-/high- level features. Table 1 shows the quantitative comparisons of LOL-real and FiveK. The proposed method achieves the best results on all metrics benefiting from the decoupled strategy. It demonstrates that enhanced images of our method are closer to ground-truth no matter in structure, color, or high-level features. Besides, we also present the comparison of model size. As shown in Table 1, the size of the proposed method is comparable to other methods.

Qualitative comparison. We present the visual results of two datasets in Fig. 8 for comparing the proposed method with some baselines good at PSNR. It can be seen that although existing methods reach decent lightness, they are hard to recover chrominance

Table 1: Quantitative comparison on the LOL-real [43] and FiveK [1]. The best results are boldfaced and the second-best ones are underlined.

Methods	LOL-real [43]					FiveK [1]					Size (M)
	PSNR ↑	SSIM ↑	ΔE_ab↓	LPIPS ↓	CSE (ratio) ↓	PSNR ↑	SSIM ↑	ΔE_ab↓	LPIPS ↓	CSE (ratio) ↓	
DRD[39]	16.08	0.6555	22.35	0.2364	2.53	21.68	0.8604	10.52	0.0574	2.18	**0.86**
Kind[52]	20.01	0.8412	12.53	0.0813	1.30	20.71	0.8835	10.75	0.0480	1.38	8.02
Kind++[51]	20.59	0.8294	12.51	0.0875	1.18	19.71	0.8640	14.05	0.0574	2.12	8.27
MIRNet[46]	<u>22.11</u>	0.7942	<u>10.11</u>	0.1448	1.35	24.41	0.9097	7.90	0.0344	<u>1.33</u>	31.79
EnGAN[8]	18.64	0.6767	17.73	0.1512	6.18	15.38	0.7752	18.89	0.0984	2.97	8.64
DeepUPE[37]	18.68	0.5791	17.54	0.1868	9.48	24.24	0.8957	8.16	0.0440	2.15	<u>0.99</u>
DeepLPF[25]	20.03	0.7819	12.58	0.1460	3.23	24.74	0.9170	7.50	0.0570	1.44	1.72
UEGAN[26]	20.30	0.7417	14.69	0.1464	12.97	23.00	0.8717	9.96	0.0503	3.84	4.16
SGM[43]	20.06	0.8158	11.36	0.0727	1.33	22.57	0.8823	9.36	0.0557	4.23	2.31
MIRNet-v2[45]	21.83	0.8455	11.47	<u>0.0666</u>	1.49	25.04	0.9188	8.05	0.0357	1.54	5.86
SNR-Aware[41]	21.48	<u>0.8478</u>	10.58	0.0740	<u>1.14</u>	<u>25.41</u>	<u>0.9234</u>	<u>7.24</u>	<u>0.0293</u>	1.49	39.12
Ours	**23.27**	**0.8637**	**8.97**	**0.0566**	**1.00**	**25.74**	**0.9285**	**6.77**	**0.0291**	**1.00**	6.84
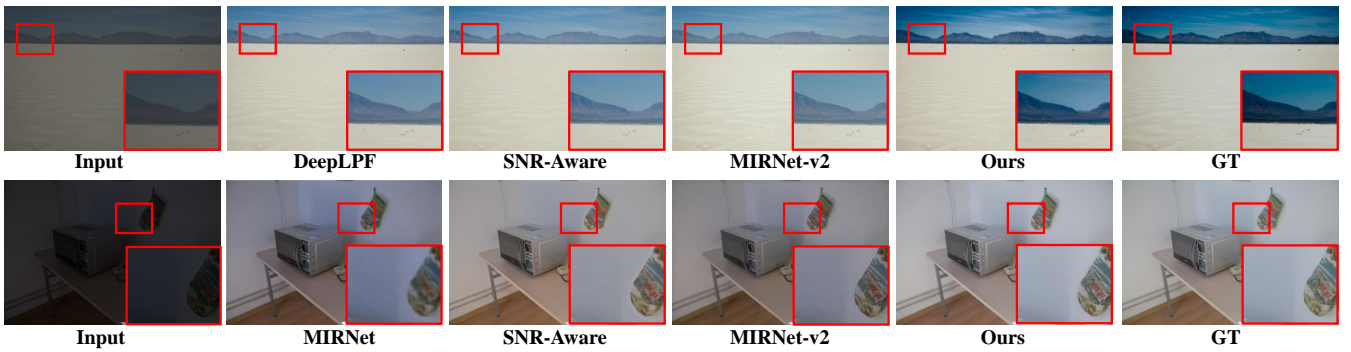
Figure 8: The qualitative comparison on FiveK [1] (the first row) and LOL-real [43] (the second row). It can be seen that the proposed method reaches the best visual results.

well (e.g., the color of the sky in Fig. 8). While the proposed method can obtain satisfying results. Besides, the proposed method achieves customized enhancement as shown in Fig. 4 and Fig. 5. The users can enhance low-light images as per their preferences.

4.3 Comparison with Two-Step "Brighten-and-Colorize" Methods

We also compare BCNet with other two-step "brighten-and-colorize" methods, which are composed of a brightener (brightening network) and a colorizer (colorization network). The brightener is an LLIE method, whose input and output are single-channel lightness. The colorizer is a user-guide image colorization method, which takes the low-light image as color hints and predicts chrominance based on the output of brightener and color hints. The implementation details of the two-step "brighten-and-colorize" can refer to Fig. 7. For brighteners, we choose SNR-Aware [41] and MIRNet-v2[45]. For colorizers, we choose an exemplar-based Yin *et al.* [44] method and a stroke-based Zhang *et al.* [50] method. Then, we pair them up to get four methods. Note that the brighteners need to be retrained on our datasets since the mismatched input/output channels of networks. The stroke-based colorizer is easy to be retrained as well. While for the exemplar-based colorizer, it is hard to be retrained in traditional LLIE datasets, since it needs to calculate similarities between the input image and the exemplar image, and query color

from the database when lacking matched colors in the exemplar image. Therefore, we opt to solely retrain the stroke-based colorizer, while utilizing the pre-trained exemplar-based colorizer.

The quantitative comparison is presented in Table 2. We adopt PSNR, SSIM, and CSE as the assessment metrics, and it can be seen that the proposed method obtains the best performance. Fig. 9 shows the qualitative results. For the exemplar-based colorizer, which aims to transfer color from the exemplar image to the input lightness, the generated color is unsaturated due to the unsaturated exemplar image (i.e., input low-light image). On the other hand, color hints in stroke-based colorization are just provided as approximate guidance. Although the input color is unsaturated, the generated color of the stroke-based colorizer is bright. After retraining, the generated color can be more realistic. For example, the input color of the Ping-Pong table in Fig. 9 is dull blue, therefore, the result of exemplar-based colorizer is still dull blue, while stroke-based colorizer can generate bright blue and retrained stroke-based colorizer can generate more realistic bright blue. However, the result of the proposed method is more accurate and saturated.

4.4 Analysis

Ablation study. We conduct the ablation study on five different settings to demonstrate the effectiveness of the proposed designs: (1) "W/o Decoupling" adopts an encoder-decoder architecture and predicts enhanced results in RGB color space; (2) "W/o Sharing" adopts

Table 2: Quantitative comparison with two-step "brighten-and-colorize" methods on LOL-real [43] dataset. The best results are boldfaced and the second-best ones are underlined. Note that "*" represents this method is retrained.

Brightener	Colorizer	PSNR ↑	SSIM ↑	CSE(ratio) ↓
SNR-Aware [41]	Zhang *et al.** [50]	20.90	0.8304	1.34
	Zhang *et al.* [50]	11.81	0.5411	70.44
	Yin *et al.* [44]	19.69	0.7881	7.40
MIRNet-v2 [45]	Zhang *et al.** [50]	21.91	0.8242	1.09
	Zhang *et al.* [50]	12.01	0.5313	77.60
	Yin *et al.* [44]	20.44	0.7810	7.30
Ours		**23.27**	**0.8637**	**1.00**

Figure 9: The qualitative comparison with "brighten-and-colorize" methods. Note that two brighteners have similar visual results, we only present the results of SNR-Aware [41].

Table 3: Ablation studies on LOL-real [43] dataset. The best results are boldfaced and the second-best ones are underlined.

Methods	PSNR ↑	SSIM ↑	CSE(ratio) ↓	Size (M)
W/o Decoupling	21.28	0.8003	3.05	4.22
W/o Sharing	23.03	0.8591	1.12	8.44
W/o LAM	22.77	0.8516	**0.91**	6.84
W/o CEM	23.06	0.8575	1.66	6.84
W/o $\mathcal{L}_q$	23.21	0.8600	1.11	6.84
Ours	**23.27**	**0.8637**	1.00	6.84

two-step "brighten-and-colorize", where brightener and colorizer are based on the proposed designs; (3) "W/o LAM" removes the lightness adjustment module; (4) "W/o CEM" removes the color embedding module and adopts concatenation; (5) "W/o $\mathcal{L}_q$" removes color classification loss.

We report the ablation study results in Table 3. We can see that our full setting yields the best PSNR, SSIM, and second-best CSE. "W/o Decoupling" verifies the effectiveness of this decoupled enhancement mode. "W/o $\mathcal{L}_q$", "W/o Sharing", "W/o LAM", and "W/o CEM" verify the effectiveness of the proposed corresponding designs. Fig. 10 presents the visual results of ablation studies. "W/o $\mathcal{L}_q$", "W/o Sharing", and "W/o CEM" hardly perform well in chrominance. "W/o LAM" may lead to worse performance in lightness. "W/o Decoupling" suffers from both above problems. Our result reaches the best visual quality. It is worth mentioning that although the quantitative results of "W/o $\mathcal{L}_q$" have only a few reductions, the qualitative result suffers from a little color vanishment (e.g., the color of grasses). It verifies the effectiveness of $\mathcal{L}_q$. Besides, we also conduct the ablation study in the other loss functions and adopted color spaces, which can be found in the supplementary materials.

Figure 10: The qualitative comparison of ablation studies.

Figure 11: Failure case. When the input image is extremely dark, we hardly predict proper chrominance, since the input image hardly provides enough chrominance information.

Limitation. The precondition of the colorization sub-task is that the chrominance of the input image contains a little color tone and shapes. However, when the input image is extremely dark, it hardly provides enough information for colorization. As a result, the chrominance of the enhanced image is very dull as shown in Fig. 11. Actually, it may be relieved by the automatic colorization methods, which is also one of our future works.

5 CONCLUSION

In this work, we novelly introduce image colorization to LLIE and propose a "brighten-and-colorize" enhancement network BCNet for low-light images. Based on the relation of image colorization and LLIE, we treat this enhancement as a multi-task learning problem. A low-light image is decomposed to lightness and chrominance and fulfills the decoupled enhancement by the proposed BCNet. BCNet contains a multi-task encoder and two task-specific decoders, which are designed elaborately according to different characteristics of lightness and chrominance. Based on the decoupled design, BCNet further achieves lightness-invariant customization with diverse saturations and color styles by manipulating the color guidance of the colorization sub-task. Extensive experiments demonstrate that BCNet sets the current SOTA results in LLIE and flexible customization. In the future, we will explore more effective ways to introduce image colorization to other image restoration tasks.

REFERENCES

[1] Vladimir Bychkovsky, Sylvain Paris, Eric Chan, and Frédo Durand. 2011. Learning photographic global tonal adjustment with a database of input/output image pairs. In *IEEE Conf. Comput. Vis. Pattern Recog.* IEEE, 97–104.

[2] Antonin Chambolle. 2004. An algorithm for total variation minimization and applications. *Journal of Mathematical Imaging and Vision* 20 (2004), 89–97.

[3] Michaël Gharbi, Jiawen Chen, Jonathan T Barron, Samuel W Hasinoff, and Frédo Durand. 2017. Deep bilateral learning for real-time image enhancement. *ACM Trans. Graph.* 36, 4 (2017), 1–12.

[4] Sergio Guadarrama, Ryan Dahl, David Bieber, Mohammad Norouzi, Jonathon Shlens, and Kevin Murphy. 2017. Pixcolor: Pixel recursive colorization. *arXiv preprint arXiv:1705.07208* (2017).

[5] Chunle Guo, Chongyi Li, Jichang Guo, Chen Change Loy, Junhui Hou, Sam Kwong, and Runmin Cong. 2020. Zero-reference deep curve estimation for low-light image enhancement. In *IEEE Conf. Comput. Vis. Pattern Recog.* 1780–1789.

[6] Mingming He, Dongdong Chen, Jing Liao, Pedro V Sander, and Lu Yuan. 2018. Deep exemplar-based colorization. *ACM Trans. Graph.* 37, 4 (2018), 1–16.

[7] Jie Huang, Yajing Liu, Feng Zhao, Keyu Yan, Jinghao Zhang, Yukun Huang, Man Zhou, and Zhiwei Xiong. 2022. Deep Fourier-Based Exposure Correction Network with Spatial-Frequency Interaction. In *Eur. Conf. Comput. Vis.* Springer, 163–180.

[8] Yifan Jiang, Xinyu Gong, Ding Liu, Yu Cheng, Chen Fang, Xiaohui Shen, Jianchao Yang, Pan Zhou, and Zhangyang Wang. 2021. Enlightengan: Deep light enhancement without paired supervision. *IEEE Trans. Image Process.* 30 (2021), 2340–2349.

[9] Zhi Jin, Muhammad Zafar Iqbal, Dmytro Bobkov, Wenbin Zou, Xia Li, and Eckehard Steinbach. 2019. A flexible deep CNN framework for image restoration. *IEEE Trans. Multimedia* 22, 4 (2019), 1055–1068.

[10] Zhi Jin, Muhammad Zafar Iqbal, Wenbin Zou, Xia Li, and Eckehard Steinbach. 2020. Dual-stream multi-path recursive residual network for JPEG image compression artifacts reduction. *IEEE Trans. Circuit Syst. Video Technol.* 31, 2 (2020), 467–479.

[11] Daniel J Jobson, Zia-ur Rahman, and Glenn A Woodell. 1997. A multiscale retinex for bridging the gap between color images and the human observation of scenes. *IEEE Trans. Image Process.* 6, 7 (1997), 965–976.

[12] Hanul Kim, Su-Min Choi, Chang-Su Kim, and Yeong Jun Koh. 2021. Representative color transform for image enhancement. In *Int. Conf. Comput. Vis.* 4459–4468.

[13] Han-Ul Kim, Young Jun Koh, and Chang-Su Kim. 2020. Global and local enhancement networks for paired and unpaired image enhancement. In *Eur. Conf. Comput. Vis.* Springer, 339–354.

[14] Han-Ul Kim, Young Jun Koh, and Chang-Su Kim. 2020. PieNet: Personalized image enhancement network. In *Eur. Conf. Comput. Vis.* Springer, 374–390.

[15] Diederik P Kingma and Jimmy Ba. 2015. Adam: A Method for Stochastic Optimization. In *Int. Conf. Learn. Represent.*

[16] Durk P Kingma and Prafulla Dhariwal. 2018. Glow: Generative flow with invertible 1x1 convolutions. *Adv. Neural Inform. Process. Syst.* 31 (2018).

[17] Manoj Kumar, Dirk Weissenborn, and Nal Kalchbrenner. 2020. Colorization Transformer. In *Int. Conf. Learn. Represent.*

[18] Wei-Sheng Lai, Jia-Bin Huang, Narendra Ahuja, and Ming-Hsuan Yang. 2018. Fast and accurate image super-resolution with deep laplacian pyramid networks. *IEEE Trans. Pattern Anal. Mach. Intell.* 41, 11 (2018), 2599–2613.

[19] Chongyi Li, Chun-Le Guo, Man Zhou, Zhexin Liang, Shangchen Zhou, Ruicheng Feng, and Chen Change Loy. 2023. Embedding Fourier for Ultra-High-Definition Low-Light Image Enhancement. *arXiv preprint arXiv:2302.11831* (2023).

[20] Xiang Li, Wenhai Wang, Xiaolin Hu, and Jian Yang. 2019. Selective kernel networks. In *IEEE Conf. Comput. Vis. Pattern Recog.* 510–519.

[21] Risheng Liu, Long Ma, Jiaao Zhang, Xin Fan, and Zhongxuan Luo. 2021. Retinex-inspired unrolling with cooperative prior architecture search for low-light image enhancement. In *IEEE Conf. Comput. Vis. Pattern Recog.* 10561–10570.

[22] Kin Gwn Lore, Adedotun Akintayo, and Soumik Sarkar. 2017. LLNet: A deep autoencoder approach to natural low-light image enhancement. *Pattern Recognition* 61 (2017), 650–662.

[23] Peng Lu, Jinbei Yu, Xujun Peng, Zhaoran Zhao, and Xiaojie Wang. 2020. Gray2colornet: Transfer more colors from reference image. In *ACM Int. Conf. Multimedia.* 3210–3218.

[24] Long Ma, Tengyu Ma, Risheng Liu, Xin Fan, and Zhongxuan Luo. 2022. Toward fast, flexible, and robust low-light image enhancement. In *IEEE Conf. Comput. Vis. Pattern Recog.* 5637–5646.

[25] Sean Moran, Pierre Marza, Steven McDonagh, Sarah Parisot, and Gregory Slabaugh. 2020. Deeplpf: Deep local parametric filters for image enhancement. In *IEEE Conf. Comput. Vis. Pattern Recog.* 12826–12835.

[26] Zhangkai Ni, Wenhan Yang, Shiqi Wang, Lin Ma, and Sam Kwong. 2020. Towards unsupervised deep image enhancement with generative adversarial network. *IEEE Trans. Image Process.* 29 (2020), 9140–9151.

[27] Qingzhe Pan, Zhifu Zhao, Xuemei Xie, Jianan Li, Yuhan Cao, and Guangming Shi. 2021. View-normalized skeleton generation for action recognition. In *ACM Int. Conf. Multimedia.* 1875–1883.

[28] Stephen M Pizer, E Philip Amburn, John D Austin, Robert Cromartie, Ari Geselowitz, Trey Greer, Bart ter Haar Romeny, John B Zimmerman, and Karel Zuiderveld. 1987. Adaptive histogram equalization and its variations. *Computer vision, graphics, and image processing* 39, 3 (1987), 355–368.

[29] Zia-ur Rahman, Daniel J Jobson, and Glenn A Woodell. 2004. Retinex processing for automatic image enhancement. *Journal of Electronic imaging* 13, 1 (2004), 100–110.

[30] Erik Reinhard, Michael Adhikhmin, Bruce Gooch, and Peter Shirley. 2001. Color transfer between images. *IEEE Computer Graphics and Applications* 21, 5 (2001), 34–41.

[31] Shaoqing Ren, Kaiming He, Ross Girshick, and Jian Sun. 2015. Faster r-cnn: Towards real-time object detection with region proposal networks. *Adv. Neural Inform. Process. Syst.* 28 (2015).

[32] Karen Simonyan and Andrew Zisserman. 2014. Very deep convolutional networks for large-scale image recognition. *arXiv preprint arXiv:1409.1556* (2014).

[33] Jheng-Wei Su, Hung-Kuo Chu, and Jia-Bin Huang. 2020. Instance-aware image colorization. In *IEEE Conf. Comput. Vis. Pattern Recog.* 7968–7977.

[34] Xiaopeng Sun, Muxingzi Li, Tianyu He, and Lubin Fan. 2021. Enhance images as you like with unpaired learning. *arXiv preprint arXiv:2110.01161* (2021).

[35] Ashish Vaswani, Noam Shazeer, Niki Parmar, Jakob Uszkoreit, Llion Jones, Aidan N Gomez, Łukasz Kaiser, and Illia Polosukhin. 2017. Attention is all you need. *Adv. Neural Inform. Process. Syst.* 30 (2017).

[36] Haolin Wang, Jiawei Zhang, Ming Liu, Xiaohe Wu, and Wangmeng Zuo. 2022. Learning Diverse Tone Styles for Image Retouching. *arXiv preprint arXiv:2207.05430* (2022).

[37] Ruixing Wang, Qing Zhang, Chi-Wing Fu, Xiaoyong Shen, Wei-Shi Zheng, and Jiaya Jia. 2019. Underexposed photo enhancement using deep illumination estimation. In *IEEE Conf. Comput. Vis. Pattern Recog.* 6849–6857.

[38] Zhou Wang, Alan C Bovik, Hamid R Sheikh, and Eero P Simoncelli. 2004. Image quality assessment: from error visibility to structural similarity. *IEEE Trans. Image Process.* 13, 4 (2004), 600–612.

[39] Chen Wei, Wenjing Wang, Wenhan Yang, and Jiaying Liu. 2018. Deep retinex decomposition for low-light enhancement. In *Brit. Mach. Vis. Conf.*

[40] Hongjun Wu, Haoran Qi, Jingzhou Luo, Yining Li, and Zhi Jin. 2022. A Lightweight Image Entropy-Based Divide-and-Conquer Network for Low-Light Image Enhancement. In *Int. Conf. Multimedia and Expo.* IEEE, 01–06.

[41] Xiaogang Xu, Ruixing Wang, Chi-Wing Fu, and Jiaya Jia. 2022. SNR-Aware Low-Light Image Enhancement. In *IEEE Conf. Comput. Vis. Pattern Recog.* 17714–17724.

[42] Bowen Yang, Chun Yang, Qi Liu, and Xu-Cheng Yin. 2019. Joint rotation-invariance face detection and alignment with angle-sensitivity cascaded networks. In *ACM Int. Conf. Multimedia.* 1473–1480.

[43] Wenhan Yang, Wenjing Wang, Haofeng Huang, Shiqi Wang, and Jiaying Liu. 2021. Sparse gradient regularized deep retinex network for robust low-light image enhancement. *IEEE Trans. Image Process.* 30 (2021), 2072–2086.

[44] Wang Yin, Peng Lu, Zhaoran Zhao, and Xujun Peng. 2021. Yes,“ Attention Is All You Need", for Exemplar based Colorization. In *ACM Int. Conf. Multimedia.* 2243–2251.

[45] SW Zamir, A Arora, SH Khan, H Munawar, FS Khan, MH Yang, and L Shao. 2022. Learning Enriched Features for Fast Image Restoration and Enhancement. *IEEE Trans. Pattern Anal. Mach. Intell.* (2022).

[46] Syed Waqas Zamir, Aditya Arora, Salman Khan, Munawar Hayat, Fahad Shahbaz Khan, Ming-Hsuan Yang, and Ling Shao. 2020. Learning enriched features for real image restoration and enhancement. In *Eur. Conf. Comput. Vis.* Springer, 492–511.

[47] Rongkai Zhang, Lanqing Guo, Siyu Huang, and Bihan Wen. 2021. ReLLIE: Deep reinforcement learning for customized low-light image enhancement. In *ACM Int. Conf. Multimedia.* 2429–2437.

[48] Richard Zhang, Phillip Isola, and Alexei A Efros. 2016. Colorful image colorization. In *Eur. Conf. Comput. Vis.* Springer, 649–666.

[49] Richard Zhang, Phillip Isola, Alexei A Efros, Eli Shechtman, and Oliver Wang. 2018. The unreasonable effectiveness of deep features as a perceptual metric. In *IEEE Conf. Comput. Vis. Pattern Recog.* 586–595.

[50] Richard Yi Zhang, Jun Yan Zhu, Phillip Isola, Xinyang Geng, Angela S Lin, Tianhe Yu, and Alexei A Efros. 2017. Real-time user-guided image colorization with learned deep priors. *ACM Trans. Graph.* 36, 4 (2017), 119.

[51] Yonghua Zhang, Xiaojie Guo, Jiayi Ma, Wei Liu, and Jiawan Zhang. 2021. Beyond brightening low-light images. *Int. J. Comput. Vis.* 129, 4 (2021), 1013–1037.

[52] Yonghua Zhang, Jiawan Zhang, and Xiaojie Guo. 2019. Kindling the darkness: A practical low-light image enhancer. In *ACM Int. Conf. Multimedia.* 1632–1640.

[53] Zhao Zhang, Huan Zheng, Richang Hong, Mingliang Xu, Shuicheng Yan, and Meng Wang. 2022. Deep Color Consistent Network for Low-Light Image Enhancement. In *IEEE Conf. Comput. Vis. Pattern Recog.* 1899–1908.

[54] Jiaojiao Zhao, Jungong Han, Ling Shao, and Cees GM Snoek. 2020. Pixelated semantic colorization. *Int. J. Comput. Vis.* 128, 4 (2020), 818–834.

[55] Suiyi Zhao, Zhao Zhang, Richang Hong, Mingliang Xu, Yi Yang, and Meng Wang. 2022. FCL-GAN: A Lightweight and Real-Time Baseline for Unsupervised Blind Image Deblurring. *arXiv preprint arXiv:2204.07820* (2022).

[56] Suiyi Zhao, Zhao Zhang, Richang Hong, Mingliang Xu, Haijun Zhang, Meng Wang, and Shuicheng Yan. 2021. Unsupervised color retention network and new quantization metric for blind motion deblurring. *TechRxiv Preprint* (2021), 1–20.

[57] Naishan Zheng, Jie Huang, Qi Zhu, Man Zhou, Feng Zhao, and Zheng-Jun Zha. 2022. Enhancement by Your Aesthetic: An Intelligible Unsupervised Personalized Enhancer for Low-Light Images. In *ACM Int. Conf. Multimedia.* 6521–6529.

Table 5: Quantitative comparison with customized LLIE methods.

Methods	PieNet [14]	Sun te al. [34]	TSFlow [36]	Ours
PSNR(dB)	25.28	20.87	25.57	25.74

Table 6: Results of the color space ablation studies on LOL-real [43] dataset. The best results are boldfaced and the second-best ones are underlined.

Methods	PSNR	SSIM	LPIPS	CSE (ratio)
HSV	22.02	0.8257	0.0809	1.12
HLS	22.31	0.8454	0.0869	1.38
Luv	22.02	0.8420	0.0702	1.06
Yuv	22.37	0.8416	0.0751	1.16
Lab (ours)	**23.21**	**0.8600**	**0.0619**	**1.00**
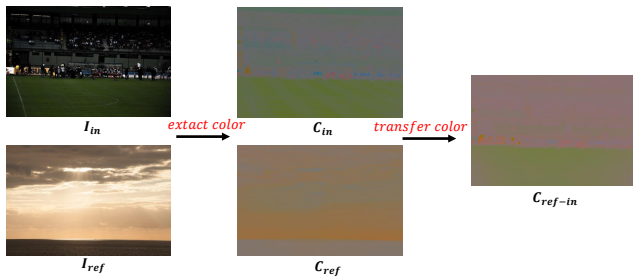
Figure 12: The process of color adaptation.
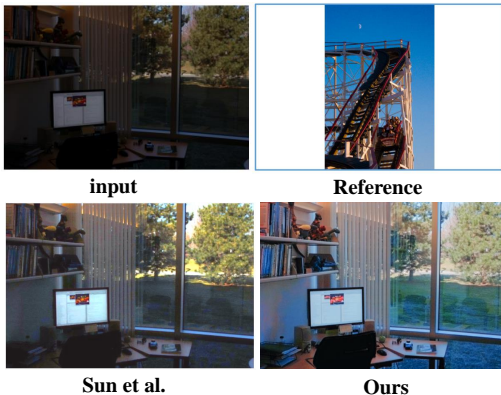
Figure 13: Visual comparison with other Su et al. [34].

Table 4: Results of the loss functions ablation studies on LOL-real [43] dataset. The best results are boldfaced and the second-best ones are underlined.

Methods	PSNR	SSIM	LPIPS	CSE (ratio)
w/o $\mathcal{L}_{ssim}$	22.40	0.8388	0.0801	1.01
w/o $\mathcal{L}_{tv}$	22.02	0.8454	0.0739	1.39
w/o $\mathcal{L}_{per}$	22.92	0.8582	0.0729	1.99
Ours	**23.27**	**0.8637**	**0.0566**	**1.00**

A ADDITIONAL ABLATION STUDIES

Loss functions. We further conduct an ablation study on loss functions.

- "W/o $\mathcal{L}_{ssim}$" removes ssim loss in brightening sub-task.
- "W/o $\mathcal{L}_{tv}$" removes smooth loss in brightening sub-task.
- "W/o $\mathcal{L}_{per}$" removes perceptual loss in colorization sub-task.

The results in Table 4 demonstrate the effectiveness of adopted loss functions.

Color spaces. In fact, there are several color spaces that can decompose an image into lightness and chrominance, such as HSV, HSI, Luv, Yuv, et al.. We conduct an ablation study on color spaces to verify the effectiveness of adopted Lab color space. However, since it is hard to quantize chrominance channels in other color spaces like [48] in Lab color space, we present the results of removing color classification loss in Lab color space for a fair comparison. As shown in Table 6, the Lab achieves the best results. Actually, it is also the popular color space in the image colorization field.

B COMPARISON WITH OTHER CUSTOMIZED LLIE METHOD

We conduct the comparison with other customized LLIE methods in Table. 5 and Fig. 13. Note that we only compare the visual result with Sun et al. [34] since only their method is based on one reference image and opens the source code. As can be seen, the proposed method reaches accurate and flexible enhancement.

C IMPLEMENTATION OF COLOR ADAPTATION

The color adaptation is responsible for generating customized color guidance based on a reference image. We utilize a non-learning method [30] to accomplish this process. Given an input low-light image I_{in} and a reference image I_{ref}, we first transform them into CIELAB color space:

$$L_{in}, a_{in}, b_{in} = RGB2Lab(I_{in})$$
$$L_{ref}, a_{ref}, b_{ref} = RGB2Lab(I_{ref}) \tag{13}$$

where $RGB2Lab(.)$ represents the color space transform function. Then, the mean value and standard deviation are used to transfer color:

$$a_{in} = a_{in} - mean(a_{in}), b_{in} = b_{in} - mean(b_{in}) \tag{14}$$

$$a_{in} = a_{in} \times (std(a_{in})/std(a_{ref}))$$
$$b_{in} = b_{in} \times (std(b_{in})/std(b_{ref})) \tag{15}$$

where $mean(.)$ and $std(.)$ represent to extract the mean value and standard deviation. Finally, the transferred color guidance $C_{ref-in} = cat(a_{in}, b_{in})$. The visual result can be seen in Fig. 12. Note that the focus of color adaptation is the chrominance information, we ignore the lightness components of two images.

D MORE VISUAL RESULTS

We present more customized enhancement results in Fig. 14 (enhancement with diverse saturations) and Fig. 15 (enhancement with diverse color styles).
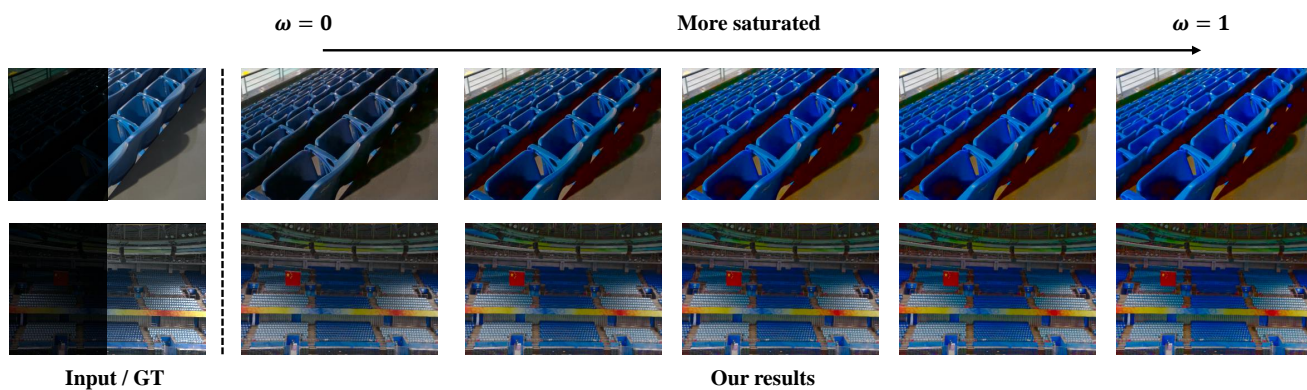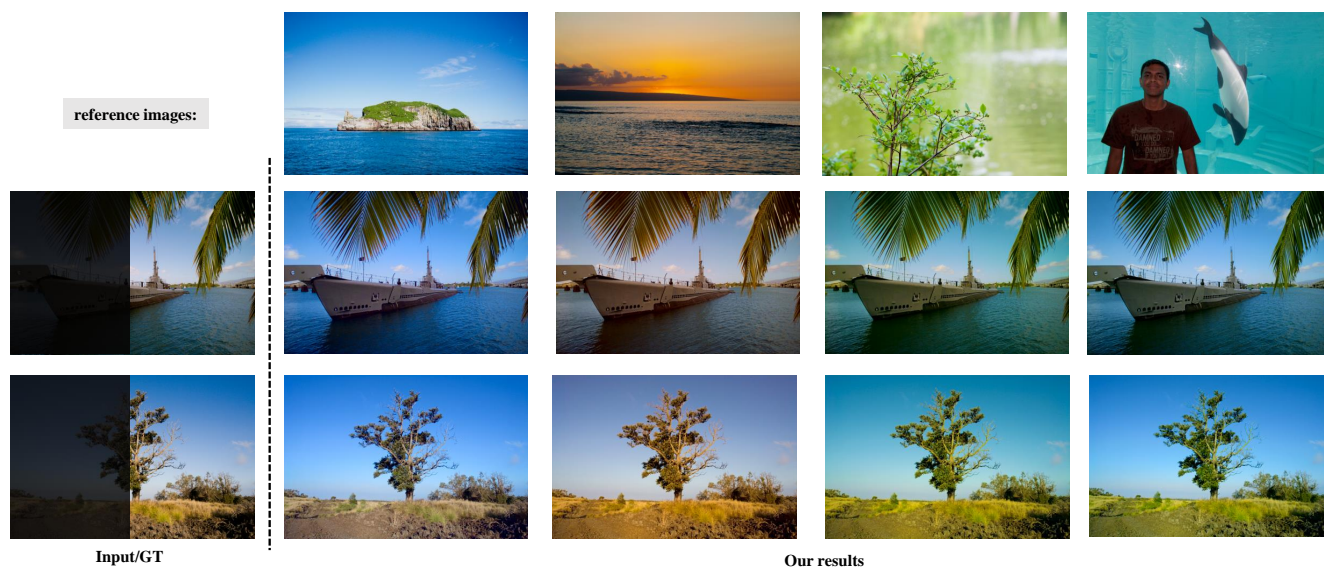
Figure 14: Enhancement with diverse saturations.

Figure 15: Enhancement with diverse color styles.